



ELSEVIER

Journal of Chromatography A, 955 (2002) 263–272

JOURNAL OF
CHROMATOGRAPHY A

www.elsevier.com/locate/chroma

Field and flow programming in frit-inlet asymmetrical flow field-flow fractionation

Myeong Hee Moon^{a,*}, P. Stephen Williams^b, Dukjin Kang^a, Inmi Hwang^a

^aDepartment of Chemistry and Chemistry Institute for Functional Materials, Pusan National University, Pusan 609-735, South Korea

^bDepartment of Biomedical Engineering, The Cleveland Clinic Foundation, 9500 Euclid Avenue, Cleveland, OH 44195, USA

Received 17 September 2001; received in revised form 28 February 2002; accepted 1 March 2002

Abstract

The separation of wide molecular mass (M_r) ranges of macromolecules using frit inlet asymmetrical flow field-flow fractionation (FI-AFIFFF) has been improved by implementing a combination of field and flow programming. In this first implementation, field strength (governed by the cross flow-rate through the membrane-covered accumulation wall) is decreased with time to obtain faster elution and improved detection of the more strongly retained (high M_r) materials. The channel outlet flow-rate is optionally held constant, increased, or decreased with time. With circulation of the flow exiting the accumulation wall to the inlet frit, the dual programming of cross flow and channel outlet flow could be implemented using just two pumps. With this flow configuration, the channel outlet flow-rate is always equal to the channel inlet flow-rate, and these may be programmed independently of the cross flow-rate through the membrane. FI-AFIFFF retains its operational advantage over conventional asymmetrical flow FFF (AFIFFF). Unlike conventional AFIFFF, FI-AFIFFF does not require time consuming, and experimentally inconvenient, sample focusing and relaxation steps involving valve switching and interruption of sample migration. The advantages of employing dual programming with FI-AFIFFF are demonstrated for sets of polystyrene sulfonate standards in the molecular mass range of 4 to 1000 kDa. It is shown that programmed FI-AFIFFF successfully expands the dynamic separation range of molecular mass. © 2002 Elsevier Science B.V. All rights reserved.

Keywords: Frit inlet asymmetrical flow field-flow fractionation; Field-flow fractionation; Dual-field and flow-programming; Hydrodynamic relaxation; Polystyrene sulfonate

1. Introduction

Field-flow fractionation (FFF) has been developed into a group of separation techniques for macromolecules and for particulates ranging from nanosize to supramicron size [1]. The programming of field

strength and/or channel flow-rate was an important step in the development of the technique. Programming was found to enhance the versatility of FFF operation so that separation time and resolution could be controlled for the more highly retained sample components. Following the first experimental work on programmed FFF, presented in conjunction with the theory of retention under programmed conditions [2], the technique has been extensively developed into a powerful tool for FFF operation [3–6]. This is especially true for sedimentation FFF,

*Corresponding author. Tel.: +82-51-510-2265; fax: +82-51-516-7421.

E-mail address: mhmoon@hyowon.pusan.ac.kr (M. Hee Moon).

where field programming is commonly utilized for the elution of broad diameter ranges of particulate materials [3,7,8]. In this technique, field strength (or rotation rate of channel) is decreased with time so that the more strongly retained particles are eluted in timely fashion. Field programming is also frequently used in thermal FFF for the faster elution of high-molecular-mass (M_r) components in the separation of broad M_r range polymers [9,10]. In flow FFF, which uses a cross flow of carrier fluid out through a semipermeable channel wall as a driving force for separation, programming has not been widely employed since its first implementation [11]. This may be due in part to the inconvenience in maintaining consistent channel flow velocity during the field (cross flow) programming of symmetrical flow FFF in which both channel walls are permeable. This was solved by circulation of carrier fluid passing out of the channel through the membrane to the inlet for the flow through the opposite, or depletion, wall. A few attempts at programmed operation of flow FFF have been made, such as in the hyperlayer separation of supramicron polystyrene standard latices using dual field and flow programming in symmetrical flow FFF [12], and in the normal mode separation of water soluble polymers using field programming in asymmetrical flow FFF [13] and symmetrical flow FFF [14,15].

In the current work, the programming technique has been applied to the frit-inlet asymmetrical flow FFF (FI-AFIFFF) channel system. Unlike the conventional flow FFF channels (both symmetrical and asymmetrical), the frit inlet asymmetrical channel operates with stopless flow injection. The sample is injected directly into the carrier stream flowing to the channel inlet. Sample relaxation is achieved hydrodynamically using the “compressive action” of a relatively high flow entering through a small frit element placed in the depletion wall close to the channel inlet [16–18]. Thus, sample injection and separation proceed without the interruption of sample migration as required by conventional relaxation procedures. Once hydrodynamic relaxation is achieved, retention of sample components in the separation segment of FI-AFIFFF channel is expected to be identical to that in a conventional asymmetrical channel.

2. Theory

We should first consider the types of programming possible in asymmetrical FIFFF, leaving aside the method of relaxation employed. For this purpose, consider a simple asymmetrical channel without a frit element flow. In this case, the flow-rate at the inlet \dot{V}_{in} contributes to the cross flow-rate through the membrane \dot{V}_c and the flow-rate at the channel outlet \dot{V}_{out} . Conservation of mass requires that:

$$\dot{V}_{in} = \dot{V}_c + \dot{V}_{out} \quad (1)$$

The channel void time t^0 , that is the time for a non retained material to pass along the length of the channel, is given by [19]:

$$t^0 = \frac{V^0}{\dot{V}_c} \ln \left(\frac{\dot{V}_{in}}{\dot{V}_{out}} \right) \quad (2)$$

where V^0 is the channel void volume. Eq. (2) requires that $\dot{V}_c > 0$, or equivalently, that $\dot{V}_{in} > \dot{V}_{out} > 0$. It should be noted that this expression for t^0 is valid for arbitrary variation of channel breadth along the channel length, or in other words, for any channel breadth profile. This includes trapezoidal [20] and exponentially [19] tapered channels.

From Eq. (1) it can be seen immediately that it is not possible to program any one of the three flow-rates without allowing at least one of the other two flow-rates to vary. It is possible to implement a programmed channel flow with constant cross flow-rate, but not a programmed cross flow-rate with constant channel flow conditions. The case of constant cross flow-rate may be implemented by programming either the inlet or the outlet flow-rate while allowing the other to vary as required by Eq. (1). The void time becomes a function of the programmed flow-rate:

$$t^0(t) = \frac{V^0}{\dot{V}_c} \ln \left(\frac{\dot{V}_{out}(t) + \dot{V}_c}{\dot{V}_{out}(t)} \right) \quad (3)$$

for programmed \dot{V}_{out} , or:

$$t^0(t) = \frac{V^0}{\dot{V}_c} \ln \left(\frac{\dot{V}_{in}(t)}{\dot{V}_{in}(t) - \dot{V}_c} \right) \quad (4)$$

for programmed \dot{V}_{in} where it is required that $\dot{V}_{in}(t) > \dot{V}_c$ for all t . Programming of channel flow alone does not provide any improvement in detectability of the strongly retained sample components. For this, one needs to program (reduce) the cross flow with time. This may be implemented with flow-rate held constant at either the channel inlet or outlet, or with a simultaneous programming of flow-rate at either channel inlet or outlet. Any of these implementations involves a dual programming of field and flow.

We can express void time as a function of time for programmed cross flow-rate and either programmed or constant outlet flow-rate as follows:

$$t^0(t) = \frac{V^0}{\dot{V}_c(t)} \ln \left(\frac{\dot{V}_{out}(t) + \dot{V}_c(t)}{\dot{V}_{out}(t)} \right) \quad (5)$$

where $\dot{V}_{out}(t)$ includes the possibility of being held constant. Similarly, for programmed cross flow-rate and either constant or programmed inlet flow-rate we have:

$$t^0(t) = \frac{V^0}{\dot{V}_c(t)} \ln \left(\frac{\dot{V}_{in}(t)}{\dot{V}_{in}(t) - \dot{V}_c(t)} \right) \quad (6)$$

where $\dot{V}_{in}(t)$ again includes the possibility of being held constant. Again it is required that $\dot{V}_{in}(t) > \dot{V}_c(t)$ for all t .

Eqs. (3)–(6) show how void time varies with time under various programmed regimes, but this is of no use in predicting retention times of retained sample components. A sample component retention time must be determined through integration of the local instantaneous zone velocity over just sufficient time for the zone to migrate to the channel outlet. It is not difficult to account for sample focusing close to the channel inlet, or for frit or split inlet sample relaxation, in all of which cases the sample migrates in quasi-equilibrium relaxed state (i.e., by the mechanism of FFF) along less than the full channel length. In the interests of simplicity for this presentation, however, we shall assume that sample components migrate along the full length of the channel. We shall consider the cases of programmed cross flow-rate with either programmed outlet flow-rate or programmed inlet flow-rate, where any of the programs include the possibility of holding the flow-rate constant.

2.1. Programmed \dot{V}_c and \dot{V}_{out}

The mean channel flow velocity as a function of distance z from the channel inlet and time t is given by:

$$\langle v \rangle(z,t) = \frac{\dot{V}_{out}(t) + \dot{V}_c(t)[1 - A(z)/A_c]}{wb(z)} \quad (7)$$

where $b(z)$ is the local channel breadth, $A(z)$ is the area of the accumulation wall from the inlet up to distance z from the inlet, and A_c is the total area of the accumulation wall. The ratio $A(z)/A_c$ may be replaced by $V(z)/V^0$, where $V(z)$ is the volume of the channel from the inlet up to point z . The local zone velocity $v_z(z,t)$ is therefore given by:

$$v_z(z,t) = R(t)\langle v \rangle(z,t) = \frac{R(t)\dot{V}_{out}(t) + R(t)\dot{V}_c(t)[1 - V(z)/V^0]}{wb(z)} \quad (8)$$

where $R(t)$ is the time dependent retention ratio which is equal to the ratio of local zone velocity v_z to local mean channel flow velocity. In symmetrical FFF, retention ratio is given by the following function of the retention parameter λ :

$$R = \frac{v_z}{\langle v \rangle} = 6\lambda[\coth(1/2\lambda) - 2\lambda] \quad (9)$$

where λ is the ratio of the mean zone layer thickness to the channel thickness, which for symmetrical flow FFF is given by:

$$\lambda = \frac{D}{|u|w} = \frac{DV^0}{w^2\dot{V}_c} \quad (10)$$

where D is the molecular diffusion coefficient, $|u|$ is the transverse flow velocity of the carrier fluid close to the membrane surface, and w is the channel thickness. The dependence of R on λ for asymmetrical FIFFF differs little from that for symmetrical FIFFF, and the difference becomes negligible at high retention [21]. The time dependence of R arises out of the dependence of λ on \dot{V}_c as shown in Eq. (10). At only moderate retention, R is given to a good approximation by:

$$R \approx 6\lambda(1 - 2\lambda) \quad (11)$$

which is accurate to 0.20% for $R < 0.6$. At strong retention the 6λ approximation for R becomes acceptable (accurate to 3.6 and 1.7% at $R=0.1$ and 0.05, respectively).

Eq. (8) may be rearranged to the form:

$$wb(z)\frac{dz}{dt} + R(t)\dot{V}_c(t)\frac{V(z)}{V^0} = R(t)\dot{V}_{out}(t) + R(t)\dot{V}_c(t) \quad (12)$$

where $v_z(z,t)$ is represented by dz/dt . At this point we may make use of the fact that $dV(z)/dz = wb(z)$ to transform the equation to:

$$\frac{dV}{dt} + R(t)\dot{V}_c(t)\frac{V}{V^0} = R(t)\dot{V}_{out}(t) + R(t)\dot{V}_c(t) \quad (13)$$

In this equation V represents the volume of the channel from the inlet up to the center of mass of the zone at time t , and dV/dt is the rate at which this volume increases with time. It is possible to simplify this equation further if the high retention approximation of 6λ is considered for R . In this case the time dependence of $R(t)\dot{V}_c(t)$ cancels, and the equation reduces to:

$$\frac{dV}{dt} + \frac{6DV}{w^2} = \frac{6DV^0}{w^2} \cdot \left(\frac{\dot{V}_{out}(t)}{\dot{V}_c(t)} + 1 \right) \quad (14)$$

and the solution of this linear differential equation is given by:

$$V = \frac{6DV^0}{w^2} \exp\left(-\frac{6Dt}{w^2}\right) \int_0^t \left(\frac{\dot{V}_{out}(t)}{\dot{V}_c(t)} + 1 \right) \exp\left(\frac{6Dt}{w^2}\right) dt \quad (15)$$

where the constant of integration must equal zero because, in our simplified presentation, the zone starts its migration from the channel inlet so that $V=0$ at $t=0$. It is also apparent that in this case V must equal V^0 at the retention time t_R . Carrying out a partial integration and rearranging results in the equation:

$$\frac{w^2}{6D} = \int_0^{t_R} \frac{\dot{V}_{out}(t)}{\dot{V}_c(t)} \exp\left(\frac{6Dt}{w^2}\right) dt \quad (16)$$

Kirkland et al. [13] presented a similar approach

to deriving an expression for retention time in programmed AFIFFF. Their derivation was restricted to channels of constant breadth and constant \dot{V}_{out} . The derivation of Eq. (16), however, is more general in that it is valid for arbitrary channel breadth profile and is not restricted to constant \dot{V}_{out} . Eqs. (14)–(16) are valid in the limit of high retention where the 6λ approximation for R holds, and this is also required for the approach presented by Kirkland et al. The approach to obtaining an accurate numerical solution for Eq. (13) will be presented elsewhere. For the assumed restrictions (constant b and \dot{V}_{out}), and a time-delayed exponential (TDE) [22,23] decay of \dot{V}_c (where the pre-decay period t_1 is set equal to the exponential decay constant τ), Kirkland et al. [13] were able to derive an analytical expression for retention time. Their solution also included the small correction for sample focusing within the channel, close to the inlet. However, we may see from the form of Eq. (16) that we could obtain an analytical expression for t_R for exponentially programmed \dot{V}_c and/or \dot{V}_{out} , and the result would be valid for arbitrary channel breadth profile. The correction for on-channel sample focusing could also be included. Any other form of program, such as linear [24,25], parabolic [2,25], or power [26], would require numerical solution of Eq. (16). Kirkland et al. identified the only program form for which an approximate analytical solution could be obtained. It must be pointed out that the existence of an approximate analytical solution for t_R does not mean that such a program is optimal for separation. The comparison of program types in terms of elution times and fractionating power is beyond the scope of the present publication.

2.2. Programmed \dot{V}_c and \dot{V}_{in}

We may carry out a similar derivation for the case of programmed \dot{V}_c and \dot{V}_{in} . The position and time dependence of $\langle v \rangle$ is now expressed in the form:

$$\langle v \rangle(z,t) = \frac{\dot{V}_{in}(t) - \dot{V}_c(t)V(z)/V^0}{wb(z)} \quad (17)$$

The derivation proceeds in the manner of the previous case, taking the 6λ approximation for R to obtain:

$$\frac{dV}{dt} + \frac{6DV}{w^2} = \frac{6DV^0}{w^2} \cdot \frac{\dot{V}_{in}(t)}{\dot{V}_c(t)} \quad (18)$$

This equation has the general solution:

$$V = \frac{6DV^0}{w^2} \exp\left(-\frac{6Dt}{w^2}\right) \int_0^t \frac{\dot{V}_{in}(t)}{\dot{V}_c(t)} \exp\left(\frac{6Dt}{w^2}\right) dt \quad (19)$$

and retention time t_R is obtained by solution of:

$$\frac{w^2}{6D} \exp\left(\frac{6Dt_R}{w^2}\right) = \int_0^{t_R} \frac{\dot{V}_{in}(t)}{\dot{V}_c(t)} \exp\left(\frac{6Dt}{w^2}\right) dt \quad (20)$$

Unlike the result for exponentially programmed \dot{V}_c and/or \dot{V}_{out} , there are no such simple programs for $\dot{V}_{in}(t)$ and $\dot{V}_c(t)$ for which an approximate analytical expression for t_R may be obtained. Eq. (20) requires numerical solution for any programmed conditions other than the specific case resulting in exponential variation of \dot{V}_c and/or \dot{V}_{out} with time.

2.3. Implementation of FI-AFIFFF

Consider the case of programmed \dot{V}_c and/or \dot{V}_{out} . To hasten the elution of the larger sample components, \dot{V}_c must be reduced with time, thereby increasing retention parameters λ and retention ratios R . An extra boost to the elution speed can be obtained by increasing \dot{V}_{out} with time. The rate at which channel volume is swept by the center of mass of a sample component is given by rearrangement of Eq. (14). This rate is given by:

$$\frac{dV}{dt}(z,t) = \frac{6DV^0}{w^2} \left(\frac{\dot{V}_{out}(t)}{\dot{V}_c(t)} + 1 \right) - \frac{6DV(z)}{w^2} \quad (21)$$

where the specific dependencies of dV/dt on z and t , and of V on z have been included. With decreasing \dot{V}_c and constant or increasing \dot{V}_{out} , Eq. (21) shows that dV/dt increases with time at all z , which is the desired result for programming. When the cross flow through the membrane is circulated to a frit element at the inlet, then \dot{V}_c is equal to frit flow-rate \dot{V}_f , and \dot{V}_{out} is equal to sample inlet flow-rate \dot{V}_s . Eq. (21) may then be written as:

$$\frac{dV}{dt}(z,t) = \frac{6DV^0}{w^2} \left(\frac{\dot{V}_s(t)}{\dot{V}_f(t)} + 1 \right) - \frac{6DV(z)}{w^2} \quad (22)$$

For a successful sample relaxation in an FI-AFIFFF channel, it has been found by experiment that the ratio of sample flow-rate \dot{V}_s to frit flow-rate \dot{V}_f should typically be less than 0.05 [16]. Eq. (22) shows that this ratio changes with time under programmed conditions. However, the ratio has to be small only at the initial conditions when the sample enters the channel and is relaxed. Once this has been achieved, the change in ratio has no influence on the separation.

Consider now the case of programmed \dot{V}_c and/or \dot{V}_{in} . Again, we expect to decrease \dot{V}_c with time, but a simultaneous increase in \dot{V}_{in} could result in too great an increase in \dot{V}_{out} and too great a reduction in resolution for the later eluting components. There may therefore be some advantage in reducing \dot{V}_{in} with time. We should examine the possible consequences. Rearrangement of Eq. (18) results in:

$$\frac{dV}{dt}(z,t) = \frac{6DV^0}{w^2} \cdot \frac{\dot{V}_{in}(t)}{\dot{V}_c(t)} - \frac{6DV(z)}{w^2} \quad (23)$$

From Eq. (23) we see that it would be disadvantageous to reduce \dot{V}_{in} more quickly than \dot{V}_c , while maintaining $\dot{V}_{in} > \dot{V}_c$ of course. All sample components would slow their elution velocities during such a program. However, if the cross flow through the membrane is circulated to the inlet frit, as proposed in this work, then $\dot{V}_{in}(t) = \dot{V}_s(t) + \dot{V}_f(t)$ and $\dot{V}_c(t) = \dot{V}_f(t)$, and the situation is once again described by Eq. (22). The holding of \dot{V}_s constant, or even allowing it to increase, is sufficient to prevent \dot{V}_{in} being reduced more quickly than \dot{V}_c . Incidentally, the holding of \dot{V}_s constant must correspond to a reduction of \dot{V}_{in} with \dot{V}_c .

In the work reported here, dual field and flow programming is applied to the FI-AFIFFF system for improving separation speed and expanding the M_r range of separation. Field programming is carried out while circulating cross flow to the inlet frit, and decreasing this circulation flow-rate with time according to a linear or power program. While cross flow-rate is decreased, sample flow-rate \dot{V}_s (or injection flow) is held constant, or is either increased or decreased linearly with time. With the circulating flow configuration, the channel outlet flow-rate \dot{V}_{out} is always equal to \dot{V}_s . Both types of program were tested for separating several polystyrene sulfonate standards in the range of 4 to 1000 kDa.

The linear program is the simplest form of programmed field or flow operation. The linear field (cross flow) decay can be expressed in the following form:

$$\dot{V}_c(t) = \dot{V}_{c0} - \Delta\dot{V}_c \left(\frac{t - t_1}{t_p} \right) \quad (24)$$

where $\dot{V}_c(t)$ is the cross flow-rate at time t , t_1 is the initial time delay, t_p is the transient time for programming, \dot{V}_{c0} is the initial cross flow-rate, and $\Delta\dot{V}_c$ is the decrease in cross flow-rate during the program [i.e., $\Delta\dot{V}_c = \dot{V}_{c0} - \dot{V}_c(t_1 + t_p)$]. Eq. (24) is valid for $t_1 \leq t \leq t_1 + t_p$. For $t < t_1$, $\dot{V}_c(t)$ is fixed at initial flow-rate \dot{V}_{c0} , and for $t > t_1 + t_p$, $\dot{V}_c(t)$ is equal to $\dot{V}_{c0} - \Delta\dot{V}_c$.

In the case of power programming, Eq. (24) is replaced by the following expression [26]:

$$\dot{V}_c(t) = \dot{V}_{c0} \left(\frac{t_1 - t_a}{t - t_a} \right)^p \quad (25)$$

where t_a is a time parameter ($t_a = -pt_1$), and p is a power usually set to 2 which is known to provide a uniform fractionating power in symmetrical flow FFF.

The linear programming of outlet flow-rate with time t can be written as:

$$\dot{V}_{out}(t) = \dot{V}_{out,0} + \Delta\dot{V}_{out} \left(\frac{t - t'_1}{p} \right) \quad (26)$$

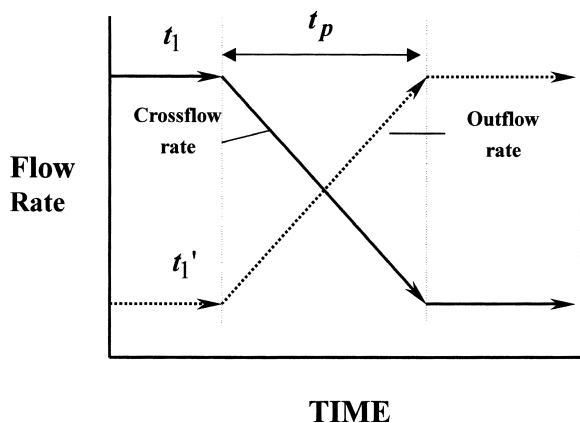


Fig. 1. Example of linear field-decay (solid line) and outlet flow-ramp (broken line) in dual programming.

where $\dot{V}_{out,0}$ represents the initial outlet flow-rate, $\Delta\dot{V}_{out}$ is the programmed change in outlet flow-rate [$= \dot{V}_{out}(t'_1 + t'_p) - \dot{V}_{out,0}$], and t'_1 and t'_p are the initial time delay and transient time for programming, respectively. Eq. (26) is valid for $t'_1 \leq t \leq t'_1 + t'_p$. Examples of field decay and increasing outlet flow-rate according to linear programs are given by the solid and broken lines in Fig. 1, respectively. For the cases shown, $t'_1 = t_1$ and $t'_p = t_p$, although this need not be so in practice.

3. Experimental

3.1. Reagents

The carrier liquid used for all of the separations presented was 0.1 M Tris-HCl buffer solution (pH 7.8) with 0.02% NaN_3 prepared from deionized water ($>18 \text{ M}\Omega/\text{cm}$). In every case this carrier solution was filtered through a membrane filter (0.45 μm pore size) prior to use. Polystyrene sulfonate (PSS) standards were obtained from American Polymer Standards (Mentor, OH, USA) having the certified weight average molecular masses in Da of 4K, 30K, 90K, 166K, 350K, and 1000K.

3.2. Apparatus

The frit inlet asymmetrical flow field-flow fractionation channel was built as described elsewhere [16–18]. The depletion wall was a Plexiglas block with the small inlet frit mounted in it, flush with the surface. The accumulation wall consisted of the usual semipermeable membrane laid over the porous frit wall mounted in a second Plexiglas block. This accumulation wall block was identical to those used in the construction of symmetrical FIFFF channels. The two blocks were clamped together around the spacer forming the channel. The channel used in this work was made using a 178 μm thick spacer. The channel breadth profile was trapezoidal, having an inlet breadth of 2.0 cm and an outlet breadth of 1.0 cm, with a tip-to-tip length of 27.2 cm. The inlet frit extended 3.0 cm from the channel inlet. A PLGC membrane was used for the accumulation wall. This

was a regenerated cellulose membrane, having an M_r cutoff of 10 kDa, from Millipore (Bedford, MA, USA).

Two high-performance liquid chromatography (HPLC) pumps were used to deliver carrier solution to the channel: a Model 305 HPLC pump from Gilson (Villers Le Bell, France) for sample injection flow and a Vintage 2000 HPLC pump from Orom-Tech (Seoul, South Korea) for frit flow. These correspond to pumps 1 and 2 of Fig. 2, respectively. For field programming, the cross outflow was connected to the inlet for frit flow, so that the flow circulated as shown in Fig. 2. A reservoir was located between the cross outflow and pump 2 in order to prevent bubble introduction to the channel and to reduce pump pulses. A needle valve was located at the channel outlet to provide back pressure and regulate flow-rates. Programming of frit flow-rate was made by using Chromastar II pump control and data acquisition software from OromTech.

Injections were made with a Model 7125 loop injector from Rheodyne (Cotati, CA, USA) having a 20 μ l loop. Eluted samples were monitored by a Shodex RI-71 differential refractometer from Showa Denko K.K. (Tokyo, Japan). Injection amounts were approximately 4–7 μ g for each PSS standard. The detector signals were recorded using the Chromastar II data acquisition software. In the case of refractive index (RI) detection during programmed runs, systematic baseline drift was observed and this was corrected for by subtracting a blank run from the PSS runs. For all runs, sample materials were injected directly into the flowing carrier stream.

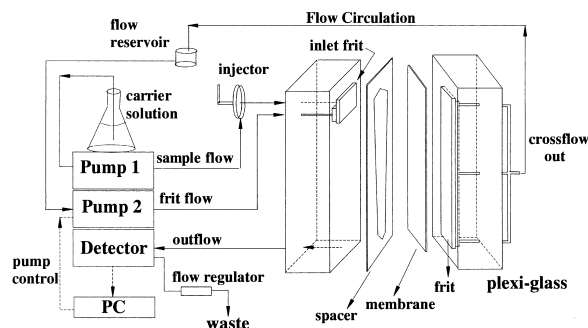


Fig. 2. System configuration for programmed FI-AFIFFF.

4. Results and discussion

Field decay in FFF is expected to result in reduced retention times. This effect is clearly demonstrated by the results shown in Figs. 3 and 4 for the separation of a PSS standard mixture. Since hydrodynamic relaxation is utilized in FI-AFIFFF, separation proceeds immediately upon sample injection, without the usual focusing/relaxation procedure of AFIFFF. For field programming in FI-AFIFFF, cross flow-rate \dot{V}_c is set equal to the frit flow-rate \dot{V}_f by circulation, as shown in Fig. 2, and therefore the resulting channel outlet flow-rate \dot{V}_{out} is identical to sample flow-rate (or injection flow-rate) \dot{V}_s . In order to demonstrate the effect of field decay alone in FI-AFIFFF, a constant field run was obtained at $\dot{V}_f = \dot{V}_c = 3.0$ ml/min and $\dot{V}_{out} = \dot{V}_s = 0.20$ ml/min. This is shown in Fig. 3. At these constant conditions, the 350 kDa PSS was eluted as a relatively broad and strongly retained peak. A high- M_r PSS (1000 kDa) was included in the mixture, but it was not seen to elute under the constant field run condition. Either the 1000 kDa PSS did not elute, or it eluted very slowly over an extended period of time and was lost in the baseline. When field programming was applied to the separation, as shown in Fig. 4a (10 min of initial time delay and 25 min transient time t_p for a linear decay of \dot{V}_c from 3.0 to 0.10 ml/min), the 166

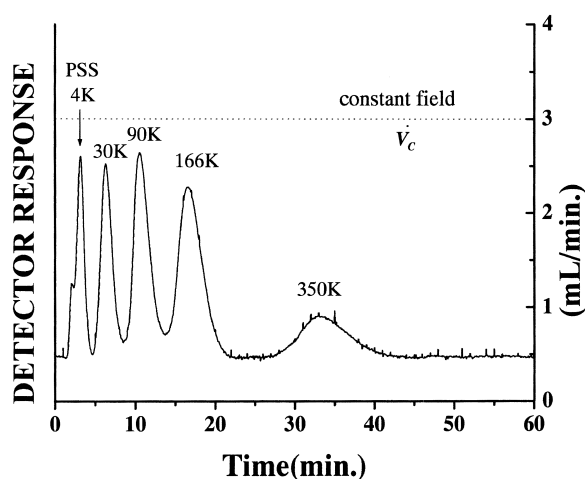


Fig. 3. Separations of PSS standards at constant field and flow conditions ($\dot{V}_f = \dot{V}_c = 3.0$ ml/min, $\dot{V}_s = \dot{V}_{out} = 0.20$ ml/min).

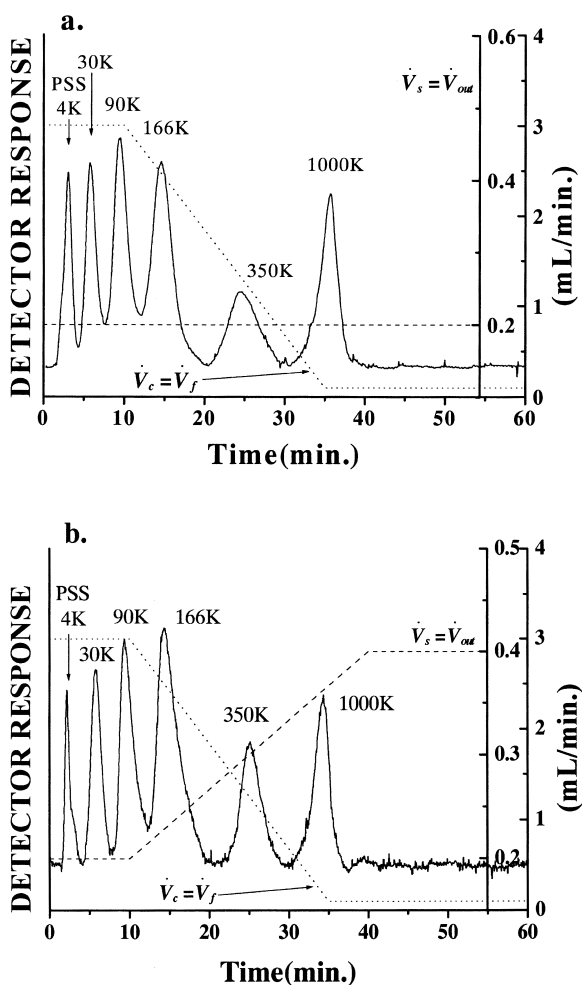


Fig. 4. Programmed separation of PSS mixture (4~1000 kDa) by linear field decay ($t_1=10$ min, $t_p=25$ min, $\dot{V}_{co}=3.0$ ml/min, $\Delta\dot{V}_c=2.9$ ml/min). (a) Constant outlet flow-rate ($\dot{V}_s=\dot{V}_{out}=0.2$ ml/min); and (b) dual field and flow programming ($t'_1=10$ min, $t'_p=30$ min, $\dot{V}_{out,0}=0.20$ ml/min, $\Delta\dot{V}_{out}=0.20$ ml/min).

and 350 kDa PSS standards eluted more quickly and their peak shapes improved. In addition, the 1000 kDa PSS was eluted under these field programming conditions. Fig. 4a shows the advantage of using field programming where the separation of very-high- M_r materials can be obtained together with low- M_r materials in the same run. As mentioned earlier, the RI signal tends to drift systematically during programming due to the change in system pressure. The fractograms shown in Fig. 4 were

baseline-corrected by subtracting blank runs obtained under identical run conditions. For these separations the initial flow-rate ratio $\dot{V}_s/\dot{V}_f=0.20/3.0=0.067$ corresponded to the constant flow-rate conditions for the separation shown in Fig. 3. This is smaller than the ratio of the areas of inlet frit and the accumulation wall (4.00 and 38.8 cm², respectively), and the sample should have been almost fully relaxed within the area of the frit inlet (see Ref. [18]). For the separation shown in Fig. 4b, programming of outlet flow-rate was added to carry out dual field and flow programming. While maintaining the same field decay pattern, outlet flow-rate starts increasing following the same time delay ($t_1=10$ min) as the field decay program, but with a transient time t_p of 30 min. The outlet flow-rate is increased linearly from 0.20 to 0.40 ml/min over this time period. The 350 kDa PSS elutes as a narrower peak in Fig. 4b. This standard elutes at very similar \dot{V}_c under the conditions of Fig. 4a and b, but it is eluted at higher outlet flow-rate in Fig. 4b. It can be assumed that the zone breadth on the channel differs somewhat for the two run conditions, and can be expected to be a little broader for the conditions of Fig. 4b where the zone is eluted at slightly faster local fluid velocities through the latter part of the channel. (Contributions to nonequilibrium zone spreading are directly dependent on mean local fluid velocity). The narrower peak for 350 kDa PSS observed in Fig. 4b results from the faster elution of the slightly broader on-channel zone by the much higher outlet flow velocity (about 0.30 ml/min as opposed to 0.20 ml/min). Though it was eluted at an increased outflow, the detectability was not significantly affected. In the case of 1000 kDa PSS, it eluted with a slightly smaller peak in Fig. 4b since it eluted at a relatively higher field strength (\dot{V}_c about 0.2 ml/min as opposed to 0.1 ml/min in Fig. 4a). The values of λ at the time of elution are therefore very different and the concentrations in outlet stream are correspondingly different. The 1000 kDa PSS peaks in Fig. 4a and b are very similar in breadth because the lowered elution retention ratio of the latter conditions is compensated by the higher \dot{V}_{out} (about 0.35 ml/min as opposed to 0.2 ml/min). It may be seen that by applying dual field and flow programming, a broad M_r (4~1000 kDa) PSS mixture can be sepa-

rated without losing efficiency or detectability.

In order to see the difference in separation efficiency under different programming patterns, a power field decay based on Eq. (25) was applied with or without the programming of channel outlet flow-rate. The three different separations shown in Fig. 5 were based on a power program having an initial delay period of 10 min with the power value of $p=2$. In Fig. 5a, power field decay is applied with a constant outlet flow-rate. Since the field decay at the beginning of power programming in Fig. 5a is steeper compared to the linear programming of Fig. 4a, the 350 kDa PSS appears less broadened and it elutes at a slightly reduced retention time. However, elution of the 1000 kDa PSS becomes more broadened and elongated in Fig. 5a since the field strength decays very slowly in the late part of power program. When ramping of outlet flow-rate was applied along with the power programmed field condition as shown in Fig. 5b, there was very little change in the elution profile observed since the outlet flow-rate started increasing after 20 min of initial delay.

In order to enhance detectability of the later eluting peaks, the outlet flow-rate was programmed in the opposite direction. When \dot{V}_{out} was programmed to decrease after an initial delay period of 20 min from 0.20 ml/min down to 0.10 ml/min as shown in Fig. 5c, the retention time of the 1000 kDa PSS increased. This is because this standard starts migrating only after the field has decayed significantly by which time the outlet flow-rate was reduced. In this case, the high- M_r component eluted at a lower field giving a higher λ value and consequently a higher sample concentration in outlet stream. The combined effect resulted in an increase of peak height and therefore detectability.

This study has shown that dual field and flow programming is advantageous for a separation of broad M_r (4~1000 kDa) water soluble polymers in a frit-inlet asymmetrical flow FFF system. Since sample injection and separation proceed without interruption of flow in FI-AFFFF, it retains its advantages over conventional channels. It is important that hydrodynamic relaxation is properly achieved to obtain the best results with dual field and flow programming.

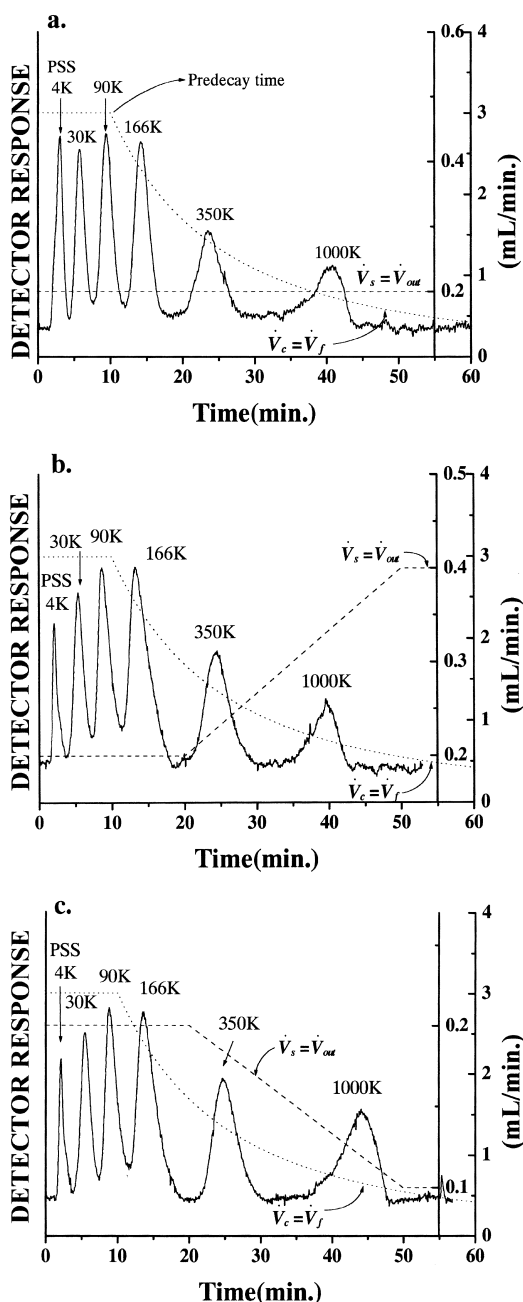


Fig. 5. Separation of PSS mixture by power programming ($t_1 = 10$ min, $t_p = -2t_1$, and $\dot{V}_{c0} = 3.0$ ml/min). (a) Field programming only, (b) dual field and flow programming by ramping up the outlet flow-rate ($t'_1 = 20$ min, $t'_p = 30$ min, $\dot{V}_{out,0} = 0.2$ ml/min, $\Delta\dot{V}_{out} = 0.2$ ml/min), and (c) dual field and flow programming by decreasing the outlet flow-rate ($t'_1 = 20$ min, $t'_p = 30$ min, $\dot{V}_{out,0} = 0.2$ ml/min, $\Delta\dot{V}_{out} = 0.1$ ml/min).

5. Nomenclature

A_f	Area of inlet frit
A_c	Total area of channel accumulation wall
$A(z)$	Area of channel accumulation wall up to point z
b	Channel breadth
$b(z)$	Local channel breadth
D	Diffusion coefficient
R	Retention ratio
$R(t)$	Time dependent retention ratio
t_1	Initial time delay
t_p	Transient time for programming
t_R	Retention time
t^0	Channel void time
$ u $	Transverse flow velocity
$V(z)$	Volume of the channel up to point z
V^0	Void volume of channel
\dot{V}_c	Cross flow-rate
\dot{V}_{c0}	Initial cross flow-rate
\dot{V}_f	Flow-rate of carrier through frit inlet
\dot{V}_{in}	Flow-rate at the inlet of asymmetrical channel
\dot{V}_{out}	Flow-rate at channel outlet
$\dot{V}_{out,0}$	Initial flow-rate at channel outlet
\dot{V}_s	Flow-rate of sample inlet substream
$\Delta\dot{V}_c$	Decrease in cross flow-rates
$\Delta\dot{V}_{out}$	Increase in outlet flow-rates
$v_z(z,t)$	Local zone velocity
$\langle v \rangle(z,t)$	Mean local flow velocity at a point z and time t
w	Channel thickness
z	Distance from channel inlet
<i>Greek characters</i>	
λ	Dimensionless retention parameter

Acknowledgements

This work was supported by Korea Research Foundation Grant (KRF-99-041-D00282).

References

- [1] M. Schimpf, K.D. Caldwell, J.C. Giddings (Eds.), *Field-Flow Fractionation Handbook*, Wiley, New York, 2000.
- [2] F.J.F. Yang, M.N. Myers, J.C. Giddings, *Anal. Chem.* 46 (1974) 1924.
- [3] P.S. Williams, J.C. Giddings, *Anal. Chem.* 59 (1987) 2038.
- [4] J.J. Kirkland, W.W. Yau, W.A. Doerner, J.W. Grant, *Anal. Chem.* 52 (1980) 1944.
- [5] K.-G. Wahlund, H.S. Winegarner, K.D. Caldwell, J.C. Giddings, *Anal. Chem.* 58 (1986) 573.
- [6] J.J. Kirkland, W.W. Yau, *J. Chromatogr.* 499 (1990) 655.
- [7] S.K.R. Williams, G.M. Raner, W.R. Ellis Jr., J.C. Giddings, *J. Microcol. Sep.* 9 (1997) 233.
- [8] W.-S. Kim, Y.H. Park, J.Y. Shin, D.W. Lee, S. Lee, *Anal. Chem.* 71 (1999) 3265.
- [9] M.N. Myers, *J. Microcol. Sep.* 9 (1997) 151.
- [10] M.N. Myers, P. Chen, J.C. Giddings, in: T. Provder (Ed.), *Chromatography of Polymers*, ACS Symposium Series No. 521, American Chemical Society, Washington, DC, 1993, p. 47.
- [11] J.C. Giddings, K.D. Caldwell, J.F. Moellmer, T.H. Dickinson, M.N. Myers, M. Martin, *Anal. Chem.* 51 (1979) 30.
- [12] S.K. Ratanathanawongs, J.C. Giddings, *Anal. Chem.* 64 (1992) 6.
- [13] J.J. Kirkland, C.H. Dilks Jr., S.W. Rementer, W.W. Yau, *J. Chromatogr.* 593 (1992) 339.
- [14] R. Hecker, P.D. Fawell, A. Jefferson, J.B. Farrow, *J. Chromatogr. A* 837 (1999) 139.
- [15] R. Hecker, P.D. Fawell, A. Jefferson, J.B. Farrow, *Sep. Sci. Technol.* 35 (2000) 593.
- [16] M.H. Moon, H. Kwon, I. Park, *Anal. Chem.* 69 (1997) 1436.
- [17] M.H. Moon, H. Kwon, I. Park, *J. Liq. Chromatogr. Rel. Technol.* 20 (1997) 2803.
- [18] M.H. Moon, P.S. Williams, H. Kwon, *Anal. Chem.* 71 (1999) 2657.
- [19] P.S. Williams, *J. Microcol. Sep.* 9 (1997) 459.
- [20] A. Litzén, K.-G. Wahlund, *Anal. Chem.* 62 (1990) 1001.
- [21] K.-G. Wahlund, J.C. Giddings, *Anal. Chem.* 59 (1987) 1332.
- [22] W.W. Yau, J.J. Kirkland, *Sep. Sci. Technol.* 16 (1981) 577.
- [23] J.J. Kirkland, S.W. Rementer, W.W. Yau, *Anal. Chem.* 53 (1981) 1730.
- [24] J.C. Giddings, L.K. Smith, M.N. Myers, *Anal. Chem.* 48 (1976) 1587.
- [25] P.S. Williams, J.C. Giddings, R. Beckett, *J. Liq. Chromatogr.* 10 (1987) 1961.
- [26] P.S. Williams, J.C. Giddings, *Anal. Chem.* 59 (1987) 2038.